Inorg. Chem. **2002**, *41*, 1299–1305

Density Functional Theory Study of Anionic and Neutral Per-Substituted 12-Vertex Boron Cage Systems, $B_{12}X_{12}^{n-}$ (n = 2, 1, 0)

Michael L. McKee[†]

Department of Chemistry, Auburn University, Auburn, Alabama 36849

Received October 1, 2001

The 12(12) closomers form a rapidly expanding class of compounds where a 12-vertex cage is surrounded by 12 identical substituents. Density functional theory (B3LYP/6-31G(d)) is used to study a number of these closomers in different states of oxidation (dianion, radical anion, and neutral cages). The cage stability increases as the group electronegativity of the substituent increases. Also, the 12(12) closomer becomes easier to oxidize as the Hammett σ_p parameter becomes more negative (electron-donating). As the closomer is oxidized, the size of the cage increases and the B–B distances become more asymmetric. The Raman-active breathing mode in the 404–434 cm^{-1} range moves to lower frequency as the cage is oxidized, which is caused by removing one or two electrons from a cage-bonding molecular orbital.

Introduction

The high symmetry of the 12-vertex $B_{12}H_{12}^{2-}$ icosahedron has always attracted attention from an aesthetic standpoint.[1] However, the interest in these 12(12) closomers[2−4] may change to more practical applications since the discovery that all 12 positions can be functionalized.[5−21] Some of the 12-vertex cages are known to exist with less than the *closo* number of cage-bonding electrons ($2n + 2$, where n = number of vertexes), in particular *hypercloso* species such as $B_{12}Cl_{12}$.[22] The usual explanation for their stability is that the exo halide substituent supplies additional electron density to the cage through π donation.

The $CB_{11}H_{12}^-$ and $C_2B_{10}H_{12}$ cages are isoelectronic to $B_{12}H_{12}^{2-}$ where a CH unit supplies the same number of cage bond electrons as BH^-. The $CB_{11}H_{12}^-$ cage and $CB_{11}X_nH_{12-n}^-$ derivatives have been exploited as nonperturbing counteranions.[23] The neutral $C_2B_{10}H_{12}$ carboranes have found application in cancer treatment where their inertness combined with a large cross section for neutron capture makes them useful in neutron capture therapy.[24,25]

[†] E-mail: mckee@chem.auburn.edu.

(1) Muetterties, E. L.; Knoth, W. H. *Polyhedral Boranes*; Marcel Dekker: New York, 1968.
(2) Closomers are defined as polyhedra whose surfaces support polyatomic substituents. The designation 12(12)-closomer indicates a polyhedron containing 12 vertexes and 12 substituents. Closomers are not dendrimers since they have a rigid polyhedral surface with many points of chain attachment.
(3) Maderna, A.; Knobler, C. B.; Hawthorne, M. F. *Angew. Chem., Int. Ed. Engl.* **2001**, *40*, 1661; **2001**, *40*, 2947 (corrigenda).
(4) Peymann, T.; Knobler, C. B.; Khan, S. I.; Hawthorne, M. F. *Angew. Chem., Int. Ed. Engl.* **2001**, *40*, 1664.
(5) Housecroft, C. E. *Angew. Chem., Int. Ed. Engl.* **1999**, *38*, 2717.
(6) Rockwell, J. J.; Herzog, A.; Peymann, T.; Knobler, C. B.; Hawthorne, M. F. *Curr. Sci.* **2000**, *78*, 405.
(7) Hawthorne, M. F. Broadening the Conflux of Boron and Carbon Chemistries. In *Contemporary Boron Chemistry*; Davidson, M. G., Hughes, A. K., Marder, T. B., Wade, K., Eds.; The Royal Society of Chemistry: Cambridge, U.K., 2000; pp 197−204.
(8) Jiang, W.; Knobler, C. B.; Mortimer, M. D.; Hawthorne, M. F. *Angew. Chem., Int. Ed. Engl.* **1995**, *34*, 1332.
(9) Jiang, W.; Knobler, C. B.; Hawthorne, M. F. *Angew. Chem., Int. Ed. Engl.* **1996**, *35*, 2536.
(10) Herzog, A.; Knobler, C. B.; Hawthorne, M. F. *Angew. Chem., Int. Ed. Engl.* **1998**, *37*, 1552.
(11) Herzog, A.; Knobler, C. B.; Hawthorne, M. F.; Maderna, A.; Siebert, W. *J. Org. Chem.* **1999**, *64*, 1045.
(12) Peymann, T.; Knobler, C. B.; Hawthorne, M. F. *Chem. Commun.* **1999**, 2039.
(13) Peymann, T.; Knobler, C. B.; Hawthorne, M. F. *Inorg. Chem.* **2000**, *39*, 1163.
(14) Peymann, T.; Knobler, C. B.; Khan, S. I.; Hawthorne, M. F. *J. Am. Chem. Soc.* **2001**, *123*, 2182.
(15) Herzog, A.; Callahan, R. P.; Macdonald, C. L. B.; Lynch, V. M.; Hawthorne, M. F.; Lagow, R. J. *Angew. Chem., Int. Ed. Engl.* **2001**, *40*, 2121.
(16) Peymann, T.; Knobler, C. B.; Khan, S. I.; Hawthorne, M. F. *Inorg. Chem.* **2001**, *40*, 1291.
(17) Thomas, J.; Hawthorne, M. F. *Chem. Commun.* **2001**, 1884.
(18) King, B. T.; Janoušek, Z.; Grüner, B.; Trammell, M.; Noll, B. C.; Michl, J. *J. Am. Chem. Soc.* **1996**, *118*, 3313.
(19) King, B. T.; Noll, B. C.; McKinley, A. J.; Michl, J. *J. Am. Chem. Chem.* **1996**, *118*, 10902.
(20) Zharov, I.; King, B. T.; Havlas, Z.; Michl, J. *J. Am. Chem. Soc.* **2000**, *122*, 10253.
(21) King, B. T.; Michl, J. *J. Am. Chem. Soc.* **2000**, *122*, 10255.
(22) McKee, M. L.; Wang, Z.-X. Wang; Schleyer, P. v. R. *J. Am. Chem. Soc.* **2000**, *122*, 4781.
(23) (a) Reed, C. A. *Acc. Chem. Res.* **1998**, *31*, 133. (b) Reed, C. A. *Acc. Chem. Res.* **1998**, *31*, 325. (c) Strauss, S. H. *Chem. Rev.* **1993**, *93*, 927.

10.1021/ic011021c CCC: $22.00
Published on Web 02/07/2002

Table 1. Experimentally Known Closomers[a]

	n ($B_{12}X_{12}^{n-}$)			n ($CB_{11}X_{12}^{n-}$)		n ($C_2B_{10}X_{12}^{n-}$)
X	2	1	0	1	0	0
OH	13, 14					
CH_3	16	12, 16		18, 20	19	8, 10, 11
$CHCl_2$						9
F^t	*b*−*e*					*f*, *g*
Cl^t	1		*h*−*m*			*n*, *o*
Br^t	1					
I^t	1, *p*−*r*					
CF_3				21, *s*		15
O_2CCH_3	13					
$O_2CC_6H_5$	13					
$O_2C(CH_2)_6$-$C_2B_{10}H_{10}(CH_3)$	17					
$OCH_2C_6H_5$	4	4	4			

[a] Numbers in the table refer to references, while letters refer to footnotes. In some cases reference is made to theoretical calculations. [b] Knoth, W. H.; Miller, H. C.; England, D. C.; Parshall, G. W.; Muetterties, E. L. *J. Am. Chem. Soc.* **1962**, *84*, 1056. [c] Knoth, W. H.; Miller, H. C.; Sauer, J. C.; Balthis, V. H.; Chia, V. T.; Muetterties, E. L. *Inorg. Chem.* **1964**, *3*, 159. [d] Solntsev, K. A.; Mebel, A. M.; Votinova, N. A.; Kuznetsov, N. T.; Charkin, O. P. *Koord. Khim.* **1992**, *18*, 340. [e] For theoretical calculations on $B_{12}F_{12}^{2-}$, see: Ionov, S. P.; Kuznetsov, N. T.; Sevast'yanov, D. V. *Russ. J. Coord. Chem.* **1999**, *25*, 689. [f] Kongpricha, S.; Schroeder, H. *Inorg. Chem.* **1969**, *8*, 2449. [g] Lagow, R. J.; Margrave, J. L. *J. Inorg. Nucl. Chem.* **1973**, *35*, 2084. [h] Lanthier, G. F.; Massey, A. G. *J. Inorg. Nucl. Chem.* **1970**, *32*, 1807. [i] Lanthier, G. F.; Kane, J.; Massey, A. G. *J. Inorg. Nucl. Chem.* **1971**, *33*, 1569. [j] Reason, M. S.; Massey, A. G. *J. Inorg. Nucl. Chem.* **1973**, *37*, 1593. [k] Reason, M. S.; Massey, A. G. *J. Inorg. Nucl. Chem.* **1976**, *38*, 1789. [l] Awad, S. A.; Prest, D. W.; Massey, A. G. *J. Inorg. Nucl. Chem.* **1978**, *40*, 395. [m] Morrison, J. A. *Chem. Rev.* **1991**, *91*, 35. [n] Schroeder, H.; Heying, T. L.; Reiner, J. R. *Inorg. Chem.* **1963**, *6*, 1092. [o] Sieckhaus, J. F.; Semenuk, N. S.; Knowles, T. A.; Schroeder, H. *Inorg. Chem.* **1969**, *8*, 2452. [p] Knoth, W. H. *J. Am. Chem. Soc.* **1966**, *88*, 936. [q] Knoth, W. H. *J. Am. Chem. Soc.* **1967**, *89*, 4850. [r] Buhrens, K.-G.; Preetz, W. *Angew. Chem., Int. Ed. Engl.* **1977**, *16*, 173. [s] For PM3 calculations on $CB_{11}(CF_3)_{12}^-$, see: Koppel, I. A.; Burk, P.; Koppel, I.; Leito, I.; Sonoda, T.; Mishima, M. *J. Am. Chem. Soc.* **2000**, *122*, 5114. [t] The halogen-substituted cages are not strictly closomers since the definition specifies polyatomic substituents.[2]

A summary of known 12(12) closomers is given in Table 1. There are five methyl 12(12) closomers, i.e., $B_{12}(CH_3)_{12}^{2-}$, $B_{12}(CH_3)_{12}^-$, $CB_{11}(CH_3)_{12}$, $CB_{11}(CH_3)_{12}$, and $C_2B_{10}(CH_3)_{12}$. The greatest range of substituents is known for $B_{12}X_{12}^{2-}$. Only two 12(12) closomers are known which deviate by two electrons from the *closo* electron count, $B_{12}Cl_{12}$ and $B_{12}(OCH_2C_6H_5)_{12}$. Three 12(12) radicals are known, $B_{12}(CH_3)_{12}^-$, $CB_{11}(CH_3)_{12}^-$, and $B_{12}(OCH_2C_6H_5)_{12}^-$.

This work will apply computational methods to the study of the 12(12) closomers. In particular, the effect of substituents on cage stability and other properties will be considered.

Computational Methods

All geometries were fully optimized in the given symmetry at the B3LYP/6-31G(d) level.[26] Vibrational frequencies, calculated at that level, determined the nature of the stationary points. Zero-point corrections are very small and have not been included unless specifically noted. Molecular plots of several closomers are shown in Figure 1.

The B3LYP/6-31G(d) geometries for boranes have been shown to be accurate and comparable to those at MP2/6-31G(d).[27] Table 2 gives the total energies (hartrees) and zero-point energies (kcal/mol) as well as other data for the closomers considered. Table S1, which contains total energies and zero-point energies of H−X and BH_2–X species where X = substituents, and Table S2, which contains the Cartesian coordinates of closomers, are provided as Supporting Information.

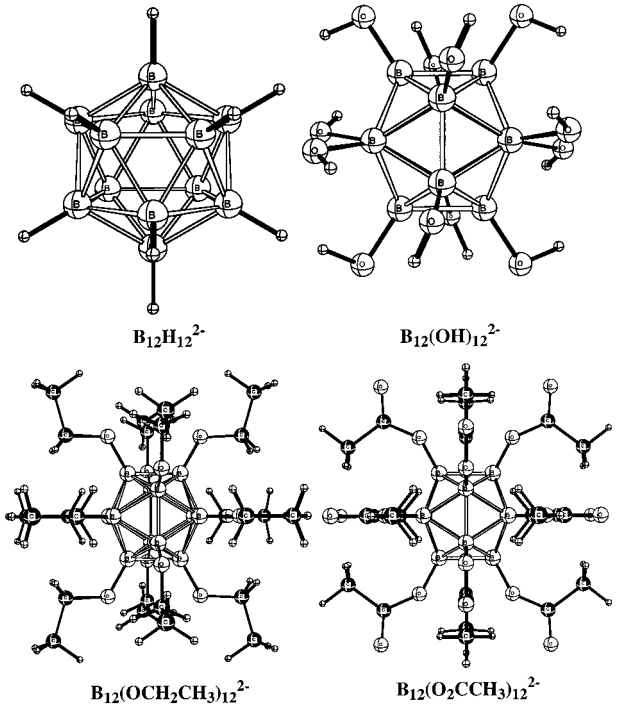

Figure 1. Molecular plots of 12(12) closomer dianions for the parent ($B_{12}H_{12}^{2-}$) and with 12 OH, OCH_2CH_3, and O_2CCH_3 substituents.

Results and Discussion

The HOMO of the $B_{12}H_{12}^{2-}$ icosahedron (I_h symmetry) is quadruply degenerate (g_u symmetry). If an electron is removed, a stabilizing molecular distortion to lower symmetry will occur according to the Jahn−Teller theorem. Several distortions are possible. In a recent study of the $B_{12}H_{12}^-$ radical anion,[22] it was found that a distortion in molecular symmetry from I_h to T_h splits the symmetry of the HOMO ($g_u \rightarrow a_u + t_u$).[28] Thus, if the a_u orbital is higher in energy than the t_u orbital, the SOMO in the radical anion would be singly degenerate (a_u) while the triple degenerate orbital (t_u) would be fully occupied with six electrons. However, alternative geometric distortions are possible. For

(24) Plešek, J. *Chem. Rev.* **1992**, *92*, 269.
(25) Soloway, A. H.; Tjarks, W.; Barnum, B. A.; Rong, F.-G.; Barth, R. F.; Codogni, I. M.; Wilson, J. G. *Chem. Rev.* **1998**, *98*, 1515.
(26) Frisch, M. J.; Trucks, G. W.; Schlegel, H. B.; Scuseria, G. E.; Robb, M. A.; Cheeseman, J. R.; Zakrzewski, V. G.; Montgomery, J. A., Jr.; Stratmann, R. E.; Burant, J. C.; Dapprich, S.; Millam, J. M.; Daniels, A. D.; Kudin, K. N.; Strain, M. C.; Farkas, O.; Tomasi, J.; Barone, V.; Cossi, M.; Cammi, R.; Mennucci, B.; Pomelli, C.; Adamo, C.; Clifford, S.; Ochterski, J.; Petersson, G. A.; Ayala, P. Y.; Cui, Q.; Morokuma, K.; Malick, D. K.; Rabuck, A. D.; Raghavachari, K.; Foresman, J. B.; Cioslowski, J.; Ortiz, J. V.; Stefanov, B. B.; Liu, G.; Liashenko, A.; Piskorz, P.; Komaromi, I.; Gomperts, R.; Martin, R. L.; Fox, D. J.; Keith, T.; Al-Laham, M. A.; Peng, C. Y.; Nanayakkara, A.; Gonzalez, C.; Challacombe, M.; Gill, P. M. W.; Johnson, B.; Chen, W.; Wong, M. W.; Andres, J. L.; Gonzalez, C.; Head-Gordon, M.; Replogle, E. S.; Pople, J. A. *Gaussian 98*; Gaussian, Inc.: Pittsburgh, PA, 1998.
(27) See: *The Encyclopedia of Computational Chemistry*; Schleyer, P. v. R., Allinger, N. L., Clark, T., Gasteiger, J., Kollman, P. A., Schaefer, H. F., III, Schreiner, P. R., Eds.; Wiley: Chichester, U.K., 1998.
(28) For a recent through discussion of the Jahn−Teller effect, see: Bersuker, I. B. *Chem. Rev.* **2001**, *101*, 1067.

Table 2. Absolute Energies (hartrees), Zero-Point Energies (kcal/mol), ^{11}B Isotropic Hyperfine Coupling Constants (MHz), and B−B and B−X Distances (Å) for Dianions, Radical Anions, and Neutral $B_{12}X_{12}$ Species

X/*n* ($B_{12}X_{12}^{n-}$)	PG	state	B3LYP/6-31G(d)	ZPE(NIF)[a]	$^{11}B_{HFCC}$[b]	BB/BB[c]	BX[c]
X = H/*n* = 2	I_h	^1A_g	−305.690 21	104.94 (0)		1.787	1.208
X = H/*n* = 1	T_h	^2A_u	−305.664 05	101.32 (0)	−0.07	1.682/1.862	1.194
X = OH/*n* = 2	T_h	^1A_g	−1208.731 64	141.43 (9)		1.783/1.791	1.456
X = OH/*n* = 2	T	^1A	−1208.739 43	146.38 (0)		1.785/1.791	1.455
X = OH/*n* = 1	T_h	^2A_u	−1208.778 96	143.99 (0)	−5.59	1.747/1.818	1.423
X = OH/*n* = 0	T_h	^1A_g	−1208.680 24	145.36 (0)		1.716/1.852	1.396
X = CH_3/*n* = 2	D_{3d}	$^1A_{1g}$	−777.544 90	315.22 (6)			
X = CH_3/*n* = 2	T_h	^1A_g	−777.545 92	315.69 (4)		1.798/1.792	1.620
X = CH_3/*n* = 2	T	^1A	−777.545 95	316.74 (0)		1.798/1.792	1.621
X = CH_3/*n* = 1	T_h	^2A_u	−777.538 91	315.08 (4)	−1.19	1.747/1.826	1.604
X = CH_3/*n* = 1	T	^2A	−777.538 92	315.86 (0)	−0.42	1.747/1.826	1.604
X = CH_3/*n* = 0	T_h	^1A_g	−777.390 54	314.79 (1)		1.702/1.870	1.589
X = CH_3/*n* = 0	T	^1A	−777.390 54	315.11 (0)		1.702/1.870	1.589
X = F/*n* = 2	I_h	^1A_g	−1497.188 56	56.24 (0)		1.793	1.393
X = F/*n* = 1	T_h	^2A_u	−1497.165 77	54.58 (0)	−6.21	1.746/1.826	1.366
X = F/*n* = 0	T_h	^1A_g	−1496.980 99	54.61 (0)		1.705/1.872	1.341
X = NH_2/*n* = 2	T_h	^1A_g	−970.088 05	233.62 (12)		1.810/1.789	1.533
X = NH_2/*n* = 2	T	^1A	−970.138 51	237.70 (0)		1.786/1.789	1.522
X = CF_3/*n* = 2	T_h	^1A_g	−4350.238 25			1.868/1.814	1.656
X = OCH_3/*n* = 2	T_h	^1A_g	−1680.363 96			1.809/1.805	1.449
X = OCH_3/*n* = 1	T_h	^2A_u	−1680.402 46		−5.57	1.777/1.827	1.422
X = OCH_3/*n* = 0	T_h	^1A_g	−1680.315 18			1.747/1.855	1.397
X = OCH_3/*n* = 0	D_{3d}	$^1A_{1g}$	−1680.276 34				
X = OCH_2CH_3/*n* = 2	T_h	^1A_g	−2152.140 68			1.807/1.805	1.448
X = O_2CH/*n* = 2	T_h	^1A_g	−2568.955 18			1.803/1.793	1.442
X = O_2CH/*n* = 0	T_h	^1A_g	−2568.600 76			1.740/1.857	1.394
X = O_2CCH_3/*n* = 2	T_h	^1A_g	−3040.749 64			1.851/1.796	1.433

[a] Zero-point energy in kcal/mol with the number of imaginary frequencies in parentheses. [b] Isotropic hyperfine coupling constants calculated at the UB3LYP/6-31G(d) level in units of MHz. [c] B−B and B−X distances in Å. There are 30 B−B bonds in the 12-vertex cage. In I_h symmetry, all bonds are the same. In T_h symmetry, there are 6 bonds of one length and 24 bonds of another length. In *T* symmetry, there are 6 bonds of one length and two sets of 12 bonds which are averaged as the second B−B distance in the table.

Table 3. Stabilization Energies (kcal/mol)

	dianion		radical anion		neutral	
X ($B_{12}X_{12}$)	eq 1	eq 2	eq 1	eq 2	eq 1	eq 2
H	0.0	0.0	0.0	0.0	0.0	0.0
OH	−155.3	297.6	−196.6	256.3	−231.0	221.9
CH_3	162.6	93.0	150.6	81.0	147.3	77.7
F	−352.7	169.2	−354.8	167.1	−335.3	186.6
OCH_3	−129.7	331.1	−170.2	290.6	−211.9	248.9
CF_3	36.0	−52.0	*a*	*a*	*a*	*a*
OCH_2CH_3	−90.9	368.0				
O_2CH	−191.5	115.2			−82.0	224.8
O_2CCH_3	−115.3	200.3	*a*	*a*	*a*	*a*
NH_2	13.4	418.9	*a*	*a*	*a*	*a*

[a] The HOMO in the dianion has t_u or t symmetry, which indicates that the radical anion and neutral systems will not have T_h or *T* symmetry.

example, if the molecular symmetry is reduced from I_h to D_{3d}, the g_u-symmetry HOMO is split into orbitals of a_{1u}, a_{2u}, and e_u symmetry.

In fact, most polyatomic exo substituents will lower the symmetry of the 12-vertex cage and split the degeneracy of the HOMO. Exo substituents having tangential lone pairs with high-lying occupied orbitals of t_u symmetry may destabilize the t_u component of the split g_u HOMO (in the dianion with T_h symmetry), pushing it above the a_u component. In these cases, removing one or two electrons will lead to a degenerate electronic state in T_h symmetry, causing the system to further distort to lower symmetry.

The effect of the exo substituent on cage stability was determined by calculating the exothermicitities of eqs 1 and 2 (Table 3).

In eq 1, a position on the 12-vertex cage is compared to a hydrogen atom, while in eq 2 the comparison is between a cage position and a BH_2 group. In eq 2, most of the reactions are quite endothermic (except X = CH_3 and CF_3), because the substituent is able to conjugate strongly with the empty p-orbital of BH_2, a stabilization mode which is not available in the cage. When X = NH_2, 12 B═N double bonds are formed in the BH_2NH_2 units which leads to the high endothermicity of 418.9 kcal/mol.[29]

$$B_{12}H_{12}^{n-} + 12HX \rightarrow B_{12}X_{12}^{n-} + 12H_2 \quad n = 2, 1, 0 \quad (1)$$

$$B_{12}H_{12}^{n-} + 12BH_2X \rightarrow B_{12}X_{12}^{n-} + 12BH_3 \quad n = 2, 1, 0 \quad (2)$$

Trends are more evident when stabilization energies from eq 1 are used. When the stabilization energies from eq 1 are

(29) For calculations on $B_{12}(NH_2)_{12}$, see: Silaghi-Dumitrescu, I.; Lara-Ochoa, F.; Bishof, P.; Haiduc, I. *THEOCHEM* **1996**, *367*, 47.

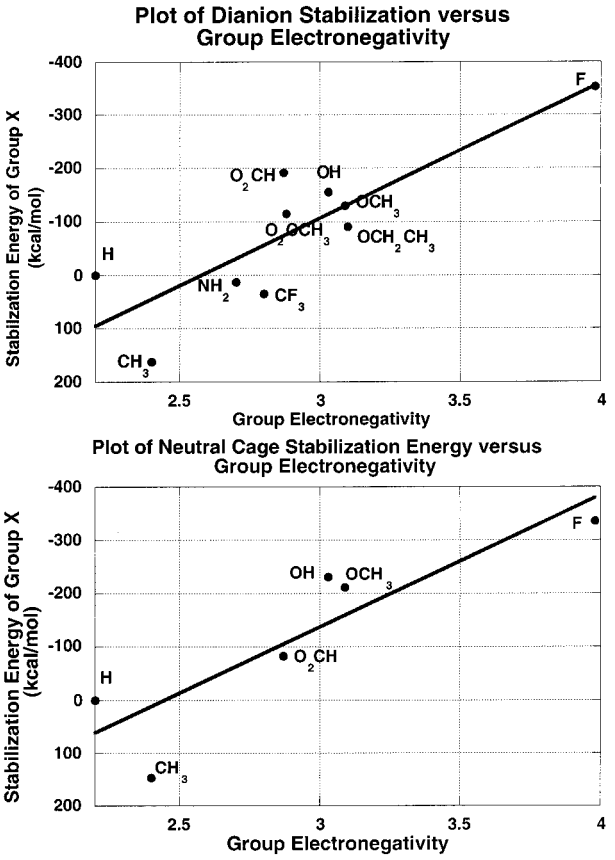

Figure 2. Plot of stabilization energy (from eq 1) versus group electronegativity[30b] for different closomers. Dianion closomers are compared above, and neutral closomers are compared below.

plotted against group electronegativites, a rough correlation (Figure 2a, dianions; Figure 2b, neutral cages) is found such that higher cage stabilities result from more electronegative substituents. The two points that deviate more in Figure 2a are CH_3 and CF_3, while the point that deviates most in Figure 2b is CH_3.

In the T_h-symmetry structure of $B_{12}(CH_3)_{12}^{2-}$, there are six H--H nonbonded distances of 2.259 Å, an indication of steric repulsion between the methyl groups. A vibrational frequency calculation reveals four imaginary modes. When the molecule is reoptimized in T symmetry, the energy is lowered by only 0.02 kcal/mol, but there are no imaginary frequencies. The methyl groups are unable to relieve much repulsion as the six close H--H nonbonded distances elongate only slightly (2.265 Å).

The exothermicity of the reaction in eq 3 was calculated to be 4.3 kcal/mol. This shows that the methyl−methyl repulsion is relatively minor in the per-substituted methyl cage.

$$12B_{12}H_{11}Me^{2-}\ (C_s\ \text{symmetry}) \rightarrow 11B_{12}H_{12}^{2-} + B_{12}Me_{12}^{2-} \quad \Delta E = 4.3\ \text{kcal/mol} \quad (3)$$

An alternative arrangement of the 12 methyl groups is possible in D_{3d} symmetry. However, the energy is 0.6 kcal/mol higher than the T symmetry (and there are 6 imaginary frequencies).

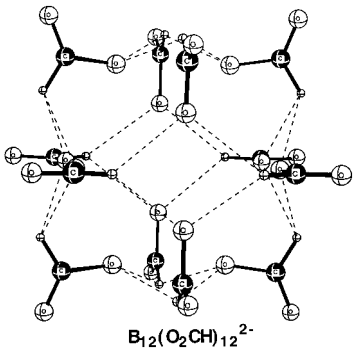

Figure 3. Molecular plots of the substituents in the $B_{12}(O_2CH)_{12}$ dianion. The boron atoms are not shown so as to emphasize the network of hydrogen bonds between OC(O)H groups.

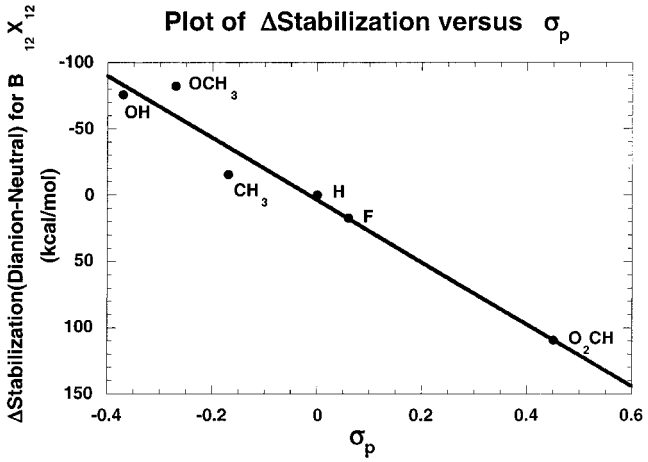

Figure 4. Plot reveals a linear relationship between Δ(stabilization) and the Hammett σ_p parameter. Δ(stabilization) is the difference in stabilization energies from eq 1 between the dianion and neutral closomer. The Hammett σ_p values are taken from ref 27b. The $B_{12}(OH)_{12}^{2-}$ and $B_{12}(OCH_3)_{12}^{2-}$ closomers are calculated to be very easy to oxidize while the $B_{12}(O_2CH)_{12}^{2-}$ closomer is predicted much more difficult to oxidize. The $B_{12}(OCH_3)_{12}^{2-}$ and $B_{12}(OCH_2Ph)_{12}^{2-}$ closomers are known to oxidize easily.[3,4]

The closomer $B_{12}(O_2CH)_{12}^{2-}$ deviates from the line toward greater stability than predicted from the linear correlation in Figure 2a. The reason can be seen in Figure 3, where only the substituents are shown (the B_{12} core is omitted). There are 24 interactions between oxygen and CH hydrogens which are absent on the reactant side of eq 1.

For six substituents, stabilization energies have been determined for the dianion and neutral cages. The difference in stabilization energy between the dianion and neutral will measure the relative ease with which the dianion may be oxidized. The parameter that correlates best is the σ_p constant from the Hammett equation (Figure 4), which measures the susceptibility to electrical effects.[30] Very electron-donating groups, such as OH and OCH_3, make the dianion easy to oxidize, while a very electron-withdrawing group, such as O_2CH, makes the dianion resistant to oxidation. In Table 4, the gas-phase adiabatic ionization energies (IP_1, IP_2, $IP_1 + IP_2$) are tabulated. For $B_{12}(OH)_{12}^{2-}$ and $B_{12}(OCH_3)_{12}^{2-}$, 1.60 and 1.33 eV are required to remove the first two electrons.

(30) (a) March, J. *Advanced Organic Chemistry*; Wiley: New York, 1985. (b) Wu, H. *Molecules* **1999**, *4*, 16. (c) Also see: http://www.unibas.ch/mdpi/ecsoc/e0002/e0002.htm.

Table 4. First and Second Adiabatic Ionization Energies (eV) for Removing Electrons from $B_{12}X_{12}^{2-}$

X ($B_{12}X_{12}^{2-}$)	IP_1	IP_2	$IP_1 + IP_2$
H	0.71	4.18	4.89
OH	−1.08	2.69	1.60
CH_3	0.19	4.04	4.23
F	0.62	5.03	5.65
OCH_3	−1.05	2.38	1.33
O_2CH			9.64

[a] A positive value indicates an endothermic process.

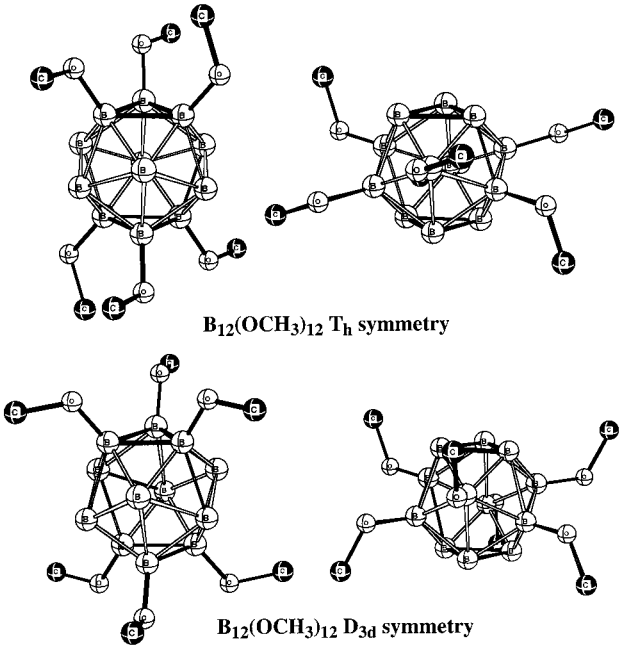

Figure 5. Molecular plots of $B_{12}(OCH_3)_{12}$ in T_h and D_{3d} point where hydrogen atoms have been omitted for clarity. The left-hand side shows the six top/bottom OCH_3 groups, while the right-hand side shows the six middle OCH_3 groups. The six top/bottom OCH_3 groups form a propeller around the C_3 axis in the T_h-symmetry structure (above left), while the six OCH_3 groups point away from the axis in the D_{3d}-symmetry structure (bottom left).

In fact, $B_{12}(OH)_{12}^{2-}$ and $B_{12}(OCH_3)_{12}^{2-}$ are predicted to be unstable to electron detachment as the first ionization energies are exothermic by 1.08 and 1.05 eV, respectively. Thus, the fact that $B_{12}(OH)_{12}^{2-}$ exists is due to stabilization effects of the medium, solvation or crystal. The closomer $B_{12}(OCH_2R)_{12}^{2-}$, where R = C_6H_5, has been made by Hawthorne and co-workers,[4] who found that the dianion could be oxidized by Fe^{III} to the radical anion and neutral cages.

It was noted that the X-ray structure of the neutral $B_{12}(OCH_2C_6H_5)_{12}$ closomer has approximate D_{3d} symmetry where the three boron atoms in the top and bottom rings had B−B distances of 1.910−1.918 Å while the remaining B−B distances were 1.755−1.864 Å.[4] The six B−O distances to the top and bottom rings were short (1.369−1.378 Å) while the other six were longer (1.398−1.404 Å). The DFT calculations (Figure 5), which were made on the neutral $B_{12}(OCH_3)_{12}$ closomer where a hydrogen replaces the phenyl group, predict the T_h-symmetry structure to be 24.4 kcal/mol more stable than the D_{3d}-symmetry structure. In addition, the asymmetry of the cage is reversed from the X-ray structure (Table 5). The top and bottom rings have the short B−B distances (1.798 Å), while the remaining B−B distances are longer (1.848 Å). Also, the boron atoms in the top and bottom ring have longer B−O distances (1.411 Å), while the middle boron atoms have shorter B−O distances (1.379 Å). The effect of the replacing hydrogen with phenyl was evaluated at the AM1 level,[31] where it was found that the optimized T_h-symmetry structure was 13.2 kcal/mol lower in energy than the optimized D_{3d}-symmetry structure. It can be concluded that both structures are similar in energy and secondary effects such as crystal packing may determine the preferred solid-state structure.

A comparison is also made in Table 5 between X-ray and DFT for other closomers. The agreement, in general, is good. As the $B_{12}(CH_3)_{12}^{2-}$ cage is oxidized to $B_{12}(CH_3)_{12}^{-}$, the B−C distance is found to decrease, both by X-ray (0.005 Å) and DFT (0.017 Å). However, there is much less asymmetry in the B−B distances in the radical anion from X-ray (0.022 Å) compared to DFT (0.079 Å).

Schleyer and co-workers have established a correlation between the asymmetry of B−B distances in the *closo* boron hydride dianions and NICS values[32] evaluated at the center of the cage.[33] The implication is that cages with large asymmetry in their B−B distances are less aromatic. In this work, one- or two-electron oxidation increases the asymmetry in the B−B distances. There is a good correlation (Figure 6) between the increase in B−B distance asymmetry (as measured by the difference between the two B−B distances in T_h symmetry) and the increase in cage size (as measured by the average B−B distances). As the anion cages are oxidized, the B−B distances become asymmetric at the same time that the average B−B distance increases. The increase in cage size is a result of removing one or two electrons from a cage bonding orbital. The increase in asymmetry is probably due to a reduction of 3-dimensional aromaticity.[33] When the substituent is OH (1-electron oxidation) or OCH_3 (2-electron oxidation), the smallest geometric effect is observed which suggests that aromaticity in these system changes little upon oxidation. On the other hand, when the substituent is H, CH_3, or F, a very large geometric effect is observed upon oxidation, suggesting a more sizable reduction in aromaticity.

(31) Dewar, M. J. S.; Zoebisch, E. G.; Healy, E. F.; Stewart, J. J. P. *J. Am. Chem. Soc.* **1985**, *107*, 3902.
(32) (a) Hofmann, M.; Schleyer, P. v. R. *Inorg. Chem.* **1999**, *38*, 652. (b) Schleyer, P. v. R.; Maerker, C.; Dransfeld, A.; Jiao, H.; Hommes, N. J. R. v. E *J. Am. Chem. Soc.* **1996**, *118*, 6317. (c) Jiao, H.; Schleyer, P. v. R. *Angew. Chem., Int. Ed. Engl.* **1996**, *35*, 2383. (d) Schleyer, P. v. R.; Jiao, H. *Pure Appl. Chem.* **1996**, *68*, 209. (e) Subramanian, G.; Schleyer, P. v. R.; Jiao, H. *Angew. Chem., Int. Ed. Engl.* **1996**, *35*, 2638. (f) Unverzagt, M.; Winkler, H. J.; Brock, M.; Hofmann, M.; Schleyer, P. v. R.; Massa, W.; Berndt, A. *Angew. Chem., Int. Ed. Engl.* **1997**, *36*, 853. (g) Schleyer, P. v. R.; Jiao, H.; Hommes, N. J. R. v. E. *J. Am. Chem. Soc.* **1997**, *119*, 12669. (h) Schleyer, P. v. R.; Najafian, K. *Inorg. Chem.* **1998**, *37*, 3454. (i) Schleyer, P. v. R.; Manoharan, M.; Wang, Z.-X.; Kiran, B.; Jiao, H.; Puchta, R.; Hommes, N. J. R. v. E. *Org. Lett.* **2001**, *3*, 2465.
(33) (a) Schleyer, P. v. R.; Subramanian, G.; Jiao, H.; Najafian, K.; Hofmann, M. In *Advances in Boron Chemistry*; Siebert, W., Ed.; Royal Society of Chemistry: Cambridge, U.K., 1997; pp 1−14. (b) Schleyer, P. v. R.; Najafian, K. Are Polyhedral Boranes, Carboranes, and Carbocations Aromatic? In *The Borane, Carborane, Carbocation Continuum*; Wiley: New York, 1998; pp 169−190.

Table 5. Experimental and Calculated Geometric Parameters (Å) for Several Closomers

	X-ray[a]		B3LYP/6-31G(d)[a]	
$X/n(B_{12}X_{12}^{n-})$	B−B	B−X	B−B	B−X
$X = H/n = 2$[b]	1.78		1.787	
$X = OH/n = 2$[c,d]	1.776−1.806	1.444	1.785−1.791	1.455
$X = CH_3/n = 2$[e]	1.785−1.807	1.611	1.792−1.798	1.621
$X = CH_3/n = 1$[e]	1.784−1.806	1.606	1.747−1.826	1.604
$X = O_2CCH_3/n = 2$[f]	1.776−1.843	1.444	1.796−1.851	1.433
$X = OCH_2R/n = 2$[g,h]	1.781−1.824	1.442	1.805−1.809	1.449
$X = OCH_2R/n = 1$[g,h]	1.768−1.840	1.408	1.777−1.827	1.422
$X = OCH_2R/n = 0$[g,h]	T/B 1.914	1.374	T/B 1.798	1.411
	middle 1.810	1.401	middle 1.848	1.379

[a] The B−B distances are the range (shortest to longest), while the B−X distance is the average. For $X = OCH_2R/n = 0$ (R = H, C_6H_5), the top B−B entry (T/B) is the B−B distance in the top and bottom three-membered ring (see Figure 5) and the bottom entry (middle) is the average of the remaining B−B distances. The top B−X entry for $X = OCH_2R$ is the B−O distances to the six boron atoms in the top and bottom three-membered rings, and the bottom B−X entry is the B−O distance to the middle six boron atoms. The calculated values for $X = OCH_2R/n = 0$ (R = H) are for the D_{3d} structure, which is 24.4 kcal/mol less stable than the T_h structure. [b] Tiritiris, I.; Schleid, T.; Müller, K.; Preetz, W. *Z. Anorg. Allg. Chem.* **2000**, *626*, 323. [c] Counterion in the X-ray structure is Rb. [d] Reference 14. [e] Reference 16. [f] Reference 13. [g] The X-ray structure corresponds to $R = C_6H_5$; the calculated structure corresponds to R = H. [h] Reference 4.

Table 6. Comparison of Two Raman-Active Modes (cm^{-1}) and Two IR-Active Modes (cm^{-1}) in $B_{12}X_{12}^{n-}$ ($n = 2, 1, 0$) Calculated at the B3LYP/6-31G(d) Level[a]

	sym	Raman active mode[b]		IR active mode[c]	
$B_{12}H_{12}^{2-}$	I_h	2569	744	1089 (1070)	710 (720)
$B_{12}H_{12}^{-}$	T_h	2673	753	956	681
$B_{12}(CH_3)_{12}^{2-}$	T	1108	427 (453)	1134 (1125)	923 (894)
$B_{12}(CH_3)_{12}^{-}$	T	1128	424	1104	959
$B_{12}(CH_3)_{12}$	T	1148	413	1124	961
$B_{12}(OH)_{12}^{2-}$	T	1266	436	1124	630
$B_{12}(OH)_{12}^{-}$	T_h	1316	433	1112	610
$B_{12}(OH)_{12}$	T_h	1370	422	1102	585
$B_{12}F_{12}^{2-}$	I_h	1315	425	1254	731
$B_{12}F_{12}^{-}$	T_h	1371	420	1230	761
$B_{12}F_{12}$	T_h	1426	404	1270	782
$B_{12}(NH_2)_{12}^{2-}$	T	1196	434	1202	704

[a] The values in parentheses are from experiment.[16] [b] Raman-active cage mode in a_{1g}, a_g, and a symmetries for I_h, T_h, and T molecular point groups, respectively. [c] IR-active cage mode in t_{1u}, t_u, and t symmetries for I_h, T_h, and T molecular point groups, respectively.

Due to the high symmetry of the 12(12) closomers, the Raman and IR spectra are simplified (Table 6). In the Raman spectra there are two breathing modes of the totally symmetric irreducible representation (a_{1g}, a_g, or a in I_h, T_h, or T point groups, respectively). An intense Raman mode was reported[16] at 453 cm^{-1} for $B_{12}(CH_3)_{12}^{2-}$, which corresponds to the calculated value of 427 cm^{-1}. A systematic increase in the Raman mode is observed upon 1- or 2-electron oxidation when the substituent is CH_3, OH, or F. In the IR spectra there are two modes that have strong to very strong intensity which are associated with cage distortions (Table 6). There does not seem to be a systematic trend as electrons are removed from a particular cage.

NICS and NMR Chemical Shifts

NICS values, the negative of the NMR absolute shielding, are known to be good indicators of aromaticity/antiaromaticity when evaluated at the center of rings or cages.[32] For example, the NICS values evaluated at the center of the boron hydride dianion cages $B_nH_n^{2-}$, $n = 6-15$, correlate with the topological resonance energy (TRE), another indicator of aromaticity.[34] NICS values were calculated for several

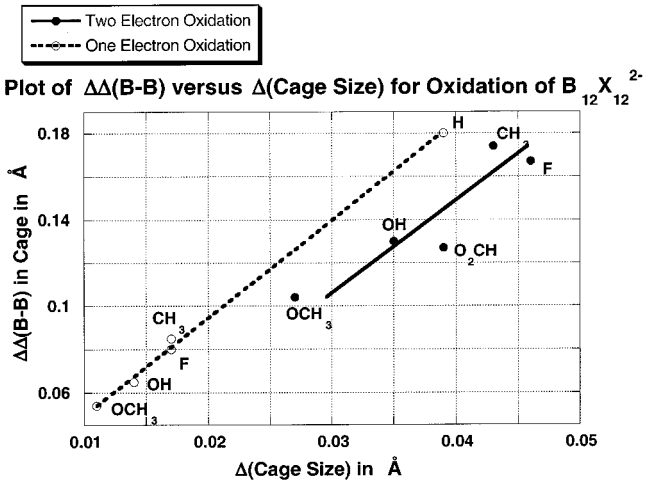

Figure 6. Plot reveals a linear relationship between increasing cage size and increasing cage asymmetry. "Cage size", the average of 30 B−B distances, is a measure of the size of the cage. Δ(cage size) is the change in the average B−B distance in the $B_{12}X_{12}^{2-}$ cage as one or two electrons are removed. Δ(B−B), the difference between the set of six B−B distances and the average of the remaining 24 B−B distances, is a measure of the asymmetry in the cage distances. ΔΔ(B−B) is a measure of the increase in asymmetry in the $B_{12}X_{12}^{2-}$ cage which occurs when one or two electrons are removed. The dashed line is for changes from dianion to radical anion closomer, while the solid line is for changes from dianion to neutral closomer.

charged and uncharged $B_{12}X_{12}$ closomers with results presented in Table 7. There is a very good relationship

(34) (a) Aihara, J. *J. Am. Chem. Soc.* **1978**, *100*, 3339. (b) Aihara, J. *J. Am. Chem. Soc.* **2001**, *40*, 5042. (c) King, R. B. *Chem. Rev.* **2001**, *101*, 1119.

Table 7. NICS Values (ppm) at the Cage Center and ^{11}B Chemical Shifts (ppm) Calculated at the GIAO/B3LYP/6-31G(d) Level for $B_{12}X_{12}$ Dianions, Radical Anions, and Neutral Species

	NICS			^{11}B chem shift[a]		
X ($B_{12}X_{12}$)	dianion	radical anion	neutral	dianion[b]	neutral	Δ
H	−25.9[c]	48.7[d]		−16.8 (−15.3)[e]		
OH	−30.5	−11.7	1.3	−15.7 (−17.1)[f]	35.9	51.6[h]
CH_3	−23.3	39.7	60.1	−12.1 (−10.8)[g]	118.1	130.2
F	−35.2	23.2	33.9	−17.0	84.3	101.3
NH_2	−27.2			−17.1		

[a] ^{11}B chemical shifts are calculated with respect to the ^{11}B chemical shift in B_2H_6 which is calculated at the same level and given a value of 16.6 ppm. [b] Experimental values are given in parentheses. [c] The NICS value is −24.6 ppm at the GIAO/B3LYP/6-31+G(d)//B3LYP/6-31G(d) level.[22] [d] The NICS value is 46.7 ppm at the GIAO/B3LYP/6-31+G(d)//B3LYP/6-31G(d) level.[22] [e] Reference 15. [f] Reference 14. [g] Reference 16. [h] There is an experimental downfield shift of 58.1 ppm in the ^{11}B resonance in $B_{12}(OCH_2Ph)_{12}$ (δ = 43.3 ppm, ref 4) relative to $[B_{12}(OCH_2Ph)_{12}]^{2-}$ (δ = −14.8 ppm, ref 4).

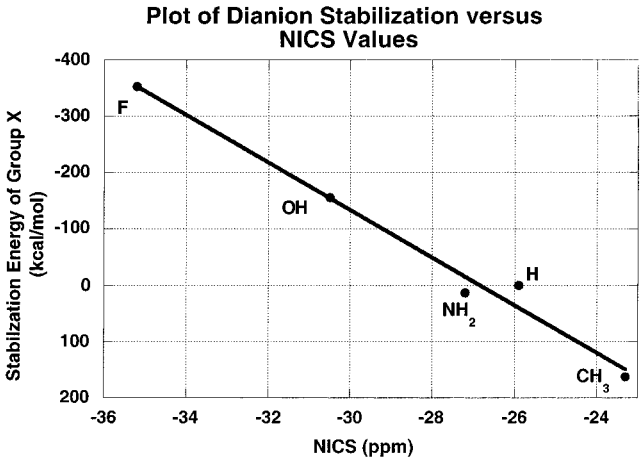

Figure 7. Plot of dianion stabilization energy (kcal/mol) from eq 1 for $B_{12}X_{12}$ dianions versus NICS values (ppm).

between the dianion NICS values and stabilization energies from eq 1 (Figure 7). The fluorine-substituted cage is predicted to be most aromatic while the methyl-substituted cage is the least aromatic.

For the radical anion cages, the NICS value for $B_{12}(OH)_{12}^-$ remains negative (−11.7 ppm, aromatic), while $B_{12}H_{12}^-$ and $B_{12}(CH_3)_{12}^-$ become positive (antiaromatic), with values of 48.7 and 39.7 ppm, respectively. For the neutral closomers, the NICS value for $B_{12}(OH)_{12}$ is very small (1.3 ppm), while the $B_{12}(CH_3)_{12}$ cage is very antiaromatic (NICS = 60.1 ppm). The calculated ^{11}B chemical shifts of the $B_{12}X_{12}^{2-}$ cages for X = H, OH, and CH_3 are in good agreement with experiment and are in the range of −11 to −17 ppm. When two electrons are removed, there is a remarkable downfield shift of the ^{11}B chemical shifts of up to 130 ppm for the $B_{12}(CH_3)_{12}^{2-}$ cage (Table 7). It is interesting to note that the calculated ^{11}B downshift shift for $B_{12}(OR)_{12}^{2-} \rightarrow B_{12}(OR)_{12}$ is 51.6 ppm for R = H, which is close to an experimental value of 58.1 ppm for R = CH_2Ph.

Conclusions

The effect of nine different substituents on the 12(12) closomers has been evaluated using density functional theory. There is a general increase in stability of the closomer as the group electronegativity increases. The ease of oxidation of the closomer dianion is related to the σ_p parameter from the Hammett equation. With the OCH_3 substituent, 2-electron oxidation is predicted to be facile, which many explain why the neutral 12(12) closomer with $OCH_2C_6H_5$ substituents was the first closomer structure to be studied by X-ray. As the 12(12) closomers are oxidized, the cage is predicted to increase in size and the B−B distances become more asymmetrical. The latter phenomena may be related to loss of aromaticity in these systems. The vibrational frequencies of the 12(12) closomers are in good agreement with the limited available experimental data.

Acknowledgment. Computer time was provided by the Alabama Supercomputer Network and the Maui High Performance Computer Center. I thank Sun Microsystems Computer Corp. for the award of an Academic Equipment Grant. I also thank Professor M. Fred Hawthorne for a helpful discussion on the closomer nomenclature.

Supporting Information Available: Absolute energies (hartrees) and zero-point energies (kcal/mol) at the B3LYP/6-31G(d) level for HX and BH_2X species (Table S1) and Cartesian coordinates for relevant structures optimized at the B3LYP/6-31G(d) level (Table S2). This material is available free of charge via the Internet at http://pubs.acs.org.

IC011021C